Available online at www.sciencedirect.com
SCIENCE DIRECT
Biochimica et Biophysica Acta 1709 (2005) 58 – 68
BIOCHIMICA ET BIOPHYSICA ACTA
BBA
http://www.elsevier.com/locate/bba

The *rpa*C gene product regulates phycobilisome–photosystem II interaction in cyanobacteria

Sarah Joshua[a], Conrad W. Mullineaux[b,*]

[a]*Department of Biology, University College London, Darwin Building, Gower Street, London WC1E 6BT, UK*
[b]*School of Biological Sciences, Queen Mary, University of London, Mile End Road, London E1 4NS, UK*

Received 25 March 2005; received in revised form 1 June 2005; accepted 19 June 2005
Available online 5 July 2005

Abstract

State transitions in cyanobacteria are a physiological adaptation mechanism that changes the interaction of the phycobilisomes with the Photosystem I and Photosystem II core complexes. A random mutagenesis study in the cyanobacterium *Synechocystis* sp. PCC6803 identified a gene named *rpa*C which appeared to be specifically required for state transitions. *rpa*C is a conserved cyanobacterial gene which was tentatively suggested to code for a novel signal transduction factor. The predicted gene product is a 9-kDa integral membrane protein. We have further examined the role of *rpa*C by overexpressing the gene in *Synechocystis* 6803 and by inactivating the ortholog in a second cyanobacterium, *Synechococcus* sp. PCC7942. Unlike the *Synechocystis* 6803 null mutant, the *Synechococcus* 7942 null mutant is unable to segregate, indicating that the gene is essential for cell viability in this cyanobacterium. The *Synechocystis* 6803 overexpressor is also unable to segregate, indicating that the cells can only tolerate a limited gene copy number. The non-segregated *Synechococcus* 7942 mutant can perform state transitions but shows a perturbed phycobilisome–Photosystem II interaction. Based on these results, we propose that the *rpa*C gene product controls the stability of the phycobilisome–Photosystem II supercomplex, and is probably a structural component of the complex.

Keywords: Cyanobacterium; Light-harvesting; Photosynthesis; Photosystem II; Phycobilisome; State transition

1. Introduction

Phycobilisomes are the main accessory light-harvesting complexes of cyanobacteria [1]. Phycobilisomes are associated with the cytoplasmic surface of the thylakoid membrane and mutational and energy transfer studies suggest that phycobilisomes can interact directly with Photosystem I (PS I) as well as Photosystem II (PS II) [2–4].

Under physiological conditions the binding of phycobilisomes to reaction centres is unstable and transient. Phycobilisomes diffuse rapidly on the thylakoid membrane surface, moving from reaction centre to reaction centre [5,6]. This mobility of phycobilisomes is important for flexibility in light-harvesting. We have shown that phycobilisome mobility is required for state transitions, a physiological adaptation mechanism that regulates the interaction of phycobilisomes with PS II and PS I [7]. Phycobilisome mobility is also involved in non-photochemical quenching in cyanobacteria grown under iron-deprivation [8]. These studies indicate that phycobilisomes can interact with several thylakoid membrane complexes: PS II, PS I and possibly also additional membrane protein complexes induced under conditions of iron-deprivation [8]. The stability of each of these phycobilisome-containing supercomplexes is likely to play a critical role in the regulation of light-harvesting.

A previous study used a genetic approach to identify a gene required for state transitions in the cyanobacterium *Synechocystis* sp. PCC6803 (*Synechocystis* 6803) [9]. A fluorescence video imaging system was used to screen a library of random, genetically-tagged mutants. Several mutants unable to perform state transitions were isolated,

* Corresponding author. Fax: +44 20 8983 0973.
E-mail address: c.mullineaux@qmul.ac.uk (C.W. Mullineaux).

0005-2728/$ - see front matter © 2005 Elsevier B.V. All rights reserved.
doi:10.1016/j.bbabio.2005.06.005

but all proved to have insertions in the same open reading-frame, designated sll1926 in CyanoBase, the on-line sequence database for *Synechocystis* 6803 (www.kazusa.or.jp/cyano/cyano.html, [10]). Based on the mutant phenotype, we designated the gene *rpa*C (Regulator of Phycobilisome Association C) [9]. *rpa*C is strongly conserved among cyanobacteria, but no significant orthologs have been detected in other organisms [11]. It codes for a putative 9 kDa integral membrane protein, with two membrane-spanning alpha-helices but no other identifiable functional domains or structural motifs [11]. The *Synechocystis* 6803 *rpa*C null mutant is unable to perform state transitions. Fluorescence spectra suggest that the mutant is permanently in State 1 (the state in which phycobilisomes preferentially associate with PS II). In all other respects, the photosynthetic apparatus of the mutant appears indistinguishable from that of the wild-type [9]. The mutant grows slower than the wild-type only under very weak illumination, particularly with yellow light which is preferentially absorbed by the phycobilisomes [9,11]. Based on these results, the *rpa*C gene product was tentatively proposed to be a novel signal transducer required for the regulation of phycobilisome–reaction centre interaction during state transitions [9]. However, it is also possible that the *rpa*C gene product might be a structural component of one of the phycobilisome–reaction centre complexes. In this case, the gene might still be essential for state transitions, but deletion would be expected to have additional effects on phycobilisome–reaction centre interaction and energy transfer.

The complete genome sequence of *Synechococcus* sp. PCC7942 (*Synechococcus* 7942) is now available on-line (US Department of Energy Joint Genome Institute: http://genome.jgi-psf.org/draft_microbes/syne1/syne1.home.html). *Synechococcus* 7942 is a well-characterised, unicellular and naturally-transformable cyanobacterium which lends itself to genetic studies on photosynthesis. It is also an excellent model organism for Fluorescence Recovery after Photobleaching (FRAP), a technique which is useful for probing the interaction of phycobilisomes and reaction centres in vivo [6,7,12]. The complete genome sequence has enabled us to identify an *rpa*C ortholog in *Synechococcus* 7942. We report a further exploration of the role of *rpa*C, based on analysis of the phenotypes of a *Synechococcus* 7942 null mutant and a *Synechocystis* 6803 overexpressor. The results suggest that the *rpa*C gene product is not a state transition signal transducer. It is more likely to be a binding factor that regulates the stability of phycobilisome–PS II interaction.

2. Material and methods

2.1. Strains and culture conditions

Wild-type *Synechococcus* sp. PCC7942 was obtained from the Pasteur Culture Collection. *Synechocystis* sp. PCC6803 (glucose-tolerant variant) was a gift from W. Vermaas (Arizona State University). Both species were grown in BG11 medium [13] supplemented with $NaHCO_3$ (10 mM). Mutants were grown in the presence of kanamycin and/or spectinomycin (50 μg/ml) as appropriate. All strains were grown in an orbital incubator at 30 °C, illuminated with white light at photon flux densities of 70, 40 or 9 μE m^{-2} s^{-1} for high, moderate or low illumination respectively, or with light defined by a blue filter ("Just Blue" from Lee Filters) at intensity 4 μE m^{-2} s^{-1}.

2.2. Molecular cloning and genotype characterisation

Routine DNA manipulations were performed according to Sambrook et al. [14]. Genomic DNA was isolated and purified from cyanobacterial cells using a standard miniprep procedure [15]. Restriction enzymes and DNA ligase were from New England BioLabs and were used with buffers recommended by the manufacturer. Polymerase Chain Reaction (PCR) was carried out using the Expand High Fidelity PCR System (Boehringer Mannheim) and products were purified with the QIAquick PCR Purification Kit (Qiagen).

The *Synechococcus* 7942 *rpa*C null mutant (Δ*rpa*C) was generated as follows. The *Synechococcus* 7942 *rpa*C ortholog (currently designated gene no. 481 on Contig 52 of the genome sequence (http://genome.jgi-psf.org/draft_microbes/synel/synel.home.html) was amplified with primers 5′-AGCGCAGCAACCATGGAACG and 5′-ATTGGTGCCTCGAGCATAGGTGC, designed to amplify a 677-bp region including the predicted coding sequence. The PCR product was cloned into pBluescript SK-(Stratagene), cut with *Bsg*1 and the ends blunted with Mung Bean nuclease. The kanamycin resistance cassette, obtained as a 1.4-kb *Hin*cII fragment from pUC4K (Pharmacia Biotech.) was ligated in, and the construct was transformed into competent *Escherichia coli* DH5α. The plasmid was used to transform *Synechococcus* 7942. Transformant colonies were selected and repeatedly restreaked on BG11 agar plates containing kanamycin. DNA was isolated and the genotype was checked using PCR with the primers listed above, plus a third primer (5′-CCTTCTTCACGAGGCAGACCTCAGCG) designed to hybridise to a sequence within the kanamycin resistance cassette.

The *Synechocystis* 6803 *rpa*C overexpressor (*Synechocystis* 6803 *rpa*C+) was generated by inserting the *rpa*C coding sequence (ORF sll1926 in the *Synechocystis* 6803 genome sequence at http://www.kazusa.or.jp/cyano/cyano.html) into the chromosomal *psb*AII locus (ORF slr1311). The *rpa*C coding sequence was amplified by PCR with primers 5′-CATACACTGCAGAGGATTTTCATATGATGG and 5′- CCTAAGATTCGGAGCTCATATGCTAGCTAACAGAG. The *Pst*1/*Sac*1 fragment excised from the PCR product was cloned into pBluescript SK^- that had been cut with the same enzymes. The construct was then digested with *Hpa*1 and ligated with a 2.1-kb spectinomycin

resistance cassette excised from pHP45ω with *Sma*I [16]. A pBluescript SK$^-$ plasmid containing the psbAII promoter region and part of its coding sequence was made in a two step procedure using primers psbA2-F1 (5′-GTCGCCCCTCTGCAGAGCCCAGAACTATG), psbA2-R1 (5′-CGCTTTCGAGCTCTTGGAGAGTCGTTGTCATATGG), psbA2-F2 (5′-GGAATTATAACCATATGACAACGACTCTC) and psbA2-R2 (5′-GTGGAGCTCTACCAACTGGTAAGGACCACC). First, the *Pst*1/*Sac*1-digested PCR product from psbA2-F1 and psbA2-R1 was cloned into pBluescript SK$^-$. The *Nde*1/*Sac*1 product from a PCR using psbA2-F2 and psbA2-R2 was cloned into the construct from the first step. The resulting construct was isolated and digested with *Nde*1. The construct containing *rpa*C and the spectinomycin resistance cassette was excised by digestion with *Nde*1 and ligated in. The complete construct was transformed into *Synechocystis* 6803 wild-type and Δ*rpa*C mutant [9] cells. Transformants were selected on spectinomycin-containing BG11 medium (50 μg/ml) and spectinomycin and kanamycin-containing medium (50 μg/ml) for the two respective mutants. Transformants were re-streaked repeatedly to encourage segregation. Genotypes were checked by PCR reactions.

A *psb*AII null mutant (Δ*psb*AII) was generated by transforming *Synechocystis* 6803 (wild-type, glucose tolerant) with a construct in which the *psb*AII gene is interrupted by a kanamycin resistance cassette. This construct was a gift from Dr. Peter Nixon (Imperial College London).

2.3. Quantification of RNA transcript levels

Total RNA was extracted from wild type and mutant cell cultures using Qiagen Protect Plant RNA Mini Kit according to the manufacturer's instructions (Qiagen), and an on-column DNase I digestion was carried out to remove DNA impurities. The concentration of RNA was determined by measuring optical density at 260 nm. The RNA was checked for integrity by gel electrophoresis on 1.5% agarose gels.

2.4. Semi-Quantitative RT-PCR

cDNA from *rpa*C mRNA was generated using 1.5 μg total RNA and the primer 5′-AGATTCTGCACTCGCTTCGA in conjunction with a reverse transcriptase kit (Qiagen). The PCR was carried out using the same primer together with 5′-ACGCTCACATTTGGCGACAT and 1/5th of the products of the RT reaction. The *psb*A1 gene encoding the D1 polypeptide of PSII was produced similarly using the primer 5′-CCGATCGGGTAGATCAGAAA with reverse transcriptase and the same primer together with 5′-GCTGTACAACGGTGGTCCTT for PCR. Primers 5′-ATGGCCAACTTCCATGGTGT and 5′-TGGGCTACACACGTACTACA were used to amplify the cDNA from the 16S ribosomal RNA transcript generated using the latter primer.

2.5. Adaptation of cells to State 1 or State 2

To adapt to state 1, cells were incubated for 5 min in 20 μE m^{-2} s^{-1} red light using a white light source equipped with a Schott RG665 filter, transmitting wavelengths of light above 665 nm. Transition to state 2 was facilitated by incubation of cells for 5 min in the dark. Freezing of cells in liquid nitrogen for fluorescence spectroscopy or treatment with high osmotic strength buffers could be carried out following adaptation to a light state.

2.6. 77K fluorescence emission spectra

Aliquots of cells suspended in BG11 to 5 μM chlorophyll were injected into silica capillary tubes of internal diameter 2.5 mm and adapted to state 1 or 2 before being frozen in liquid nitrogen. Emission spectra were obtained by placing these tubes in the liquid nitrogen housing of a Perkin Elmer LS50 Luminescence Spectrophotometer (Foster City, CA) equipped with a red-sensitive photomultiplier. Excitation and emission slit widths were set at 5 nm, and for excitation of phycobilins and chlorophyll, spectra were recorded between 620 nm and 750 nm for excitation at 600 nm and 435 nm, respectively.

2.7. Room-temperature fluorescence timecourses

To observe state transitions at room temperature, 3 ml of cells suspended to a concentration of 10 μM chlorophyll and placed in a cuvette in the LS50 luminescence spectrometer. With slit widths set to 10 nm and excitation light at 600 nm, fluorescence at 680 nm was recorded over a 600-s period. Cells were kept in darkness except between 150 s and 450 s when given red-illumination using the same intensity red light described in 2.6 above.

2.8. Quantification of pigments and photosystems

Chlorophyll concentration was estimated by methanol extraction and absorbance at 665 nm [17]. Phycocyanin and chlorophyll concentrations were also obtained from cell absorption spectra using the formulae of Myers et al. [18]. PS II was estimated by a ^{14}C-atrazine binding assay [19]. Cells at 20 μM chlorophyll were incubated for 3 min in darkness in the presence of different concentrations of ^{14}C-atrazine. Following centrifugation, the supernatants containing unbound atrazine were mixed with scintillation cocktail (Sigma-Fluor) and counted in a scintillation counter. ^{14}C-atrazine concentrations were estimated using known concentrations as a reference. PSII content is given by the amount of atrazine bound at saturating atrazine concentration, and this was estimated using a weighted linear regression of the reciprocals of atrazine added versus the reciprocal of atrazine bound. SigmaPlot (Jandel Scientific, San Rafael, CA) software was used. PS I concentration was determined using flash photo-oxidation of P_{700}, in a lab-

built spectrophotometer (Peter Rich, University College London). Cells at 10 μM chlorophyll were incubated for 15 s in the dark in the presence of 50 μM DCMU. The cells received eight saturating 6 μs flashes of blue light generated using a BG39 filter (Schott) over a white light source in order to completely oxidise P_{700} of PS I. The red wavelength detection was generated using a 695 nm cut-on filter and a narrow band 695–703 nm notch filter. 8 measurements were averaged. PSI content was determined from the flash-induced absorbance difference, using a P_{700} extinction coefficient of 64 mM^{-1} cm^{-1} [20].

2.9. Oxygen evolution

Oxygen evolution was recorded at increasing light intensities using an OxyLab 2 oxygen electrode (Hansatech, King's Lynn) equipped with red light-emitting diodes. Oxygen evolution rates were averaged from three replicate measurements. No electron acceptors were added.

2.10. Treatment with high osmotic strength solutions

Cells suspended to 50 μM chlorophyll in BG11 were pre-adapted to state 1 or state 2 before being re-suspended to 5 μM chlorophyll in 0.5 M sucrose. The illumination conditions were maintained for a further 5 min and then aliquots were maintained in the same state or alternately adapted before being frozen in capillary tubes for fluorescence spectroscopy. For FRAP studies, aliquots of sucrose-treated cells were adsorbed onto 1.5% agar plates containing 0.5 M sucrose.

2.11. FRAP measurements

Cells were adsorbed onto 1.5% agar plates made with BG11, sucrose or phosphate buffer following adaptation and fixation to state 1 or 2 where appropriate. A sample of BG11 agar, which the cells had been adsorbed to, was transferred to a sample holder and covered with a 0.2-mm glass coverslip. The sample holder was connected to a circulating water bath maintained at 30 °C.

The measurements were carried out using a PCM2000 laser-scanning confocal microscope (Nikon, Tokyo). For observation of phycobilisomes, a 20-mW red He–Ne laser (633 nm) was used, with fluorescence emission above 665 nm selected with a Schott RG665 filter. Cells were observed using a 60× oil-immersion objective lens, with pinhole size of 50 μm.

The laser scanned over an area of 20.5 × 20.5 μm, and a cell aligned along the *y*-axis could be imaged by reducing the intensity of the laser by a factor of 8 with a neutral density filter. At time 0 s, the laser power was increased for 2 s in order to bleach chromophores in a narrow region along the *x*-axis of the cell. Image series were recorded over appropriate timescales depending on the speed of pigment diffusion.

2.12. FRAP data analysis

Diffusion coefficients were determined from the series of images as previously described [5,6,12]. A one-dimensional fluorescence profile was extracted for pre- and post-bleach images using Optimas 5.2 image analysis software. The post-bleach data were subtracted from the pre-bleach profile and the resultant profiles fitted to Gaussian curves using SigmaPlot (Jandel Scientific, San Rafael, CA). Linear regression of bleach depths versus time allows an estimation of the diffusion coefficient according to a diffusion equation described previously [5]. Averages and standard deviations of diffusion coefficients obtained from at least six cells were obtained.

3. Results

3.1. The Synechococcus 7942 chromosome contains a single rpaC ortholog

The predicted amino-acid sequence of *Synechocystis* 6803 RpaC (the product of ORF sll1926) was used in a BLAST search against the *Synechococcus* 7942 genome sequence (http://genome.jgi-psf.org/draft_microbes/synel/synel.home.html). These sequence data were produced by the US Department of Energy Joint Genome Institute (http://www.jgi.doe.gov/). The search identified a single significant match, an ORF currently annotated as gene 481 on Contig 52, coding for a hypothetical protein. The predicted product of gene 481 is a protein of 104 amino-acids, showing 67% identity and 86% similarity with *Synechocystis* 6803 RpaC (Fig. 1) Both gene products have two predicted transmembrane alpha-helices. The transmembrane regions and the N-terminal sequence (predicted to be on the cytoplasmic side of the membrane) are particularly strongly conserved, and this is true of all the cyanobacterial RpaC orthologs [11]. The predicted *Synechococcus* 7942 gene product has a C-terminal extension as compared to *Synechocystis* 6803 RpaC (Fig. 1). The *Synechococcus* 7942 gene has no close downstream neighbours, the next predicted ORF beginning 591 bases downstream (not shown).

```
MMERDLPKYRMVCTLSFGDIYGQIIVWLIVIFLSLASALALASSTRPVYALATVGLVLVLSLPFLLFSFVTTIFNHLDFVPVESD
  MDRLKRYRVACTLTFGDIYGQIITWIIVILLSLAAALALMGAQQPIYALTTVGLILVVSLPFLLFAFVTTILNHIELRPLEASAESSTTTPAELSFSNPAINPS
```

Fig. 1. Alignment of predicted amino-acid sequences for RpaC from *Synechocystis* 6803 (top) and *Synechococcus* 7942 (bottom). N-terminus is to the left and boxes indicate predicted transmembrane alpha-helices. *Synechocystis* 6803 sequence data were produced by the Kazusa DNA Research Institute, Japan, and *Synechococcus* 7942 sequence data were produced by the US Department of Energy Joint Genome Institute (http://www.jgi.doe.gov/).

3.2. *rpaC* is essential for viability in *Synechococcus* 7942

We set out to construct a *Synechococcus* 7942 null mutant. A construct was created in which a portion of the *rpa*C coding sequence was excised with *Bsg*I and replaced with a kanamycin resistance cassette. DNA from kanamycin-resistant transformants was analysed by PCR. Products of the predicted sizes were obtained from transformant DNA, but a PCR product corresponding to that from the wild-type was also obtained (not shown). Repeated re-streaking did not lead to loss of the wild-type PCR product, whether the cells were grown in high, moderate or low white light, or in blue light. This clearly indicates that the transformant is unable to segregate, and therefore that complete loss of the *rpa*C gene is lethal under a wide range of illumination conditions.

3.3. The partially-segregated *Synechococcus* 7942 Δ*rpaC* mutant shows lower *rpaC* transcript levels

Semi-quantitative RT-PCR was used to compare *rpa*C mRNA transcript levels in the wild-type and the partially-segregated mutant. Transcript levels for *psb*A1 and 16SrRNA were used as standards. Total RNA was extracted from cultures grown under moderate illumination conditions. cDNAs were generated by reverse transcription with appropriate primers and known quantities of RNA, and this was followed by PCR amplification. Extractions, reverse transcription and PCR were repeated in triplicate. Gel photographs for one replicate for each gene are shown in Fig. 2. The results indicate that:

(i.) 16SrRNA is much higher relative to total RNA in the mutant than in the wild-type.
(ii.) *psb*A1 transcripts levels are significantly higher relative to total RNA in the mutant than in the wild-type.
(iii.) *rpa*C transcript levels are much lower relative to total RNA, and relative to *psb*A1 RNA, in the mutant than in the wild-type.

The detection of *rpa*C transcripts confirms that the mutant is non-segregated. The much lower *rpa*C transcript levels suggest a lower level of *rpa*C expression in the mutant, and this is the only obvious explanation for the strong phenotypic effect of the mutation (see below). The effect on *psb*A1 transcript levels is consistent with the higher PSII content in the mutant (see below).

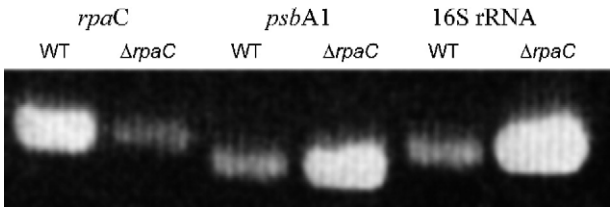

Fig. 2. *rpa*C and *psb*A1 expression in *Synechococcus* 7942 Δ*rpa*C. Semi-quantitative RT-PCR analysis of *rpa*C and *psb*A1 transcripts, and 16S rRNA from Δ*rpa*C and wild-type. PCR products amplified from cDNA obtained from equal total quantities of RNA.

3.4. Phenotypic characterisation of the non-segregated *Synechococcus* 7942 Δ*rpaC* mutant

Δ*rpa*C cells were grown under moderate illumination. Cell absorption spectra were used to check levels of chlorophyll and phycocyanin, which showed no significant differences from wild-type cells grown under the same conditions (Table 1).

Mutant cells showed a much greater range of cell lengths than wild-type cells, and were significantly longer on average than wild-type cells. The average mutant cell length was 11.8 ± 6.5 μm, as compared to 8.4 ± 3.5 μm for the wild-type. The difference is significant ($P < 4 \times 10^{-4}$). Stress conditions have been previously shown to cause elongation of *Synechococcus* 7942 cells [21].

Photosystem I content was quantified by flash photolysis, and was found to be similar in the wild-type and in Δ*rpa*C (Table 1). Photosystem II was quantified using an atrazine-binding assay. PSII content per cell was nearly twice as high in Δ*rpa*C as in the wild-type (Table 1) and 77K fluorescence spectra showed higher relative PSII fluorescence (Table 1). Oxygen evolution under saturating red light was similar in wild-type and the mutant (not shown).

Table 2 shows the mean doubling times for Δ*rpa*C and wild-type in liquid culture under a range of illumination conditions. Δ*rpa*C is significantly disadvantaged as compared to the wild-type under high light, but not under other growth conditions.

3.5. The non-segregated *Synechococcus* 7942 Δ*rpaC* mutant is capable of state transitions but shows perturbed phycobilisome–PSII energy transfer

Fluorescence emission spectra recorded at 77K can be used to assess the efficiency of energy transfer from the phycobilisomes to the reaction centres [22] and also to show the effects of state transitions [9]. Typical spectra obtained with phycocyanin excitation are shown in Fig. 3. The peak at 650 nm is from phycocyanin, while the peak at 685 nm comes both from the long-wavelength "terminal emitters" of the phycobilisome core, and from PS II. The 695 nm shoulder is from PS II and the 720 nm peak is from PS I [9]. Adaptation to State 1 conditions increases PS II emission in the mutant as well as in the wild-type (Fig. 3) indicating that the mutant is still capable of state transitions. Fluorescence timecourses recorded at room temperature (Fig. 3) confirm that the non-segregated Δ*rpa*C mutant is capable of state transitions. Exposure of cells to light preferentially absorbed by PS I results in a fluorescence increase characteristic of the transition to State 1, and removal of this light results in an immediate fluorescence rise due to PSII trap closure,

Table 1
Pigment contents of *Synechococcus* 7942 and *Synechocystis* 6803 strains grown under moderate illumination

	Synechococcus 7942		*Synechocystis* 6803	
	Wild-type	Δ*rpa*C	Δ*psbAII*	Δ*rpa*C.*rpa*C+
Phycocyanin/cell	$(6.3\pm0.3)\times10^7$	$(7.9\pm2.6)\times10^7$	$(2.7\pm0.04)\times10^7$	$(2.5\pm0.3)\times10^7$
Chlorophyll/cell	$(1.0\pm0.1)\times10^8$	$(1.3\pm0.4)\times10^8$	$(6.8\pm0.02)\times10^7$	$(3.5\pm0.03)\times10^7$
Phycocyanin/Chlorophyll	0.63±0.05	0.59±0.01	0.32±0.01	0.71±0.01
PSII/cell	122,000±6000	206,000±9000	173,000±3000	210,000±1000
PSI/cell	420,000	490,000	521,000	233,000
PSI/PSII	3.4	2.4	3.0	1.1
F_{PSI}/F_{PSII}	1.8	1.6	3.7	2.2

For pigments and photosystems, absolute numbers per cell are presented. Phycocyanin and chlorophyll per cell were obtained from absorption spectra, PSII per cell was obtained from a ^{14}C-atrazine binding assay and PSI per cell was obtained from flash photolysis of P_{700} (details in Materials and methods). F_{PSI}/F_{PSII} is the ratio of PSI to PSII fluorescence peaks in fluorescence spectra recorded at 77K with 435 nm (chlorophyll) excitation. F_{PSII} was at 695 nm and F_{PSI} was at 725 nm (*Synechocystis* 6803) or 718 nm (*Synechococcus* 7942).

followed by a fall in fluorescence characteristic of the transition to State 2 [9]. However, the 77K fluorescence spectra (Fig. 3) show that the mutant consistently has lower fluorescence at 695 nm as compared to 685 nm. This suggests a lower efficiency of energy transfer from phycobilisomes to Photosystem II [22].

3.6. The non-segregated *Synechococcus* 7942 Δ*rpa*C mutant shows weaker coupling of phycobilisomes to Photosystem II

We have previously used Fluorescence Recovery after Photobleaching (FRAP) to probe the interaction of phycobilisomes with reaction centres in *Synechococcus* 7942 in vivo [6,7]. A laser-scanning confocal microscope is used to visualise image fluorescence from the photosynthetic pigments (either phycobilisomes or the chlorophylls of Photosystem II). The highly-focused confocal laser spot is then used to bleach the chromophores in a line across the cell. The subsequent spread of the line and recovery of fluorescence in the centre of the line allow quantitative estimates of the diffusion coefficient of the fluorophore [5–7,12]. The technique can be applied quantitatively to any cyanobacteria with elongated cells and a regular thylakoid membrane conformation, including *Synechococcus* 7942 [6,7,12]. Photosystem II normally appears completely immobile in wild-type *Synechococcus* 7942 [18]. We obtained a similar result in Δ*rpa*C (not shown). In contrast to Photosystem II, the phycobilisomes usually diffuse rather rapidly on the membrane surface [6] indicating that the coupling of phycobilisomes to reaction centres is weak and reversible [5,6].

Table 2
Mean doubling times in exponential phase for *Synechococcus* 7942 and *Synechocystis* 6803 strains under different illumination conditions (white light unless otherwise specified)

Strain	Illumination conditions	Mean doubling time (h)
Synechococcus 7942 WT	High	9±3
Synechococcus 7942 Δ*rpa*C	High	18±6
Synechococcus 7942 WT	Moderate	26±9
Synechococcus 7942 Δ*rpa*C	Moderate	24±13
Synechococcus 7942 WT	Low	35±7
Synechococcus 7942 Δ*rpa*C	Low	45±5
Synechococcus 7942 WT	Blue	71±6
Synechococcus 7942 Δ*rpa*C	Blue	74±8
Synechocystis 6803 Δ*psb*AII	High	13±2
Synechocystis 6803 Δ*rpa*C	High	13±2
Synechocystis 6803 Δ*rpa*C.*rpa*C+	High	24±8
Synechocystis 6803 Δ*psb*AII	Moderate	11.4±0.1
Synechocystis 6803 Δ*rpa*C	Moderate	12.0±0.04
Synechocystis 6803 Δ*rpa*C.*rpa*C+	Moderate	23±2
Synechocystis 6803 Δ*psb*AII	Low	34±2
Synechocystis 6803 Δ*rpa*C	Low	35±1
Synechocystis 6803 Δ*rpa*C.*rpa*C+	Low	49±1
Synechocystis 6803 Δ*psb*AII	Blue	72±4
Synechocystis 6803 Δ*rpa*C	Blue	75±5
Synechocystis 6803 Δ*rpa*C.*rpa*C+	Blue	72±1

See Materials and methods for the light intensities used.

FRAP measurements provide a way to assess the stability of phycobilisome–reaction centre interaction: a more stable interaction will result in slower phycobilisome diffusion, and vice versa. We have demonstrated this in *Synechococcus* 7942 using artificial conditions which stabilise phycobilisome–reaction centre interaction. Under these conditions, the diffusion of phycobilisomes is drastically slowed [7].

We used FRAP to probe phycobilisome mobility in Δ*rpa*C. In wild-type cells we obtained a mean phycobilisome diffusion coefficient of $(4.80\pm2.11)\times10^{-10}$ cm^2 s^{-1}. In Δ*rpa*C cells grown under the same conditions we obtained a mean phycobilisome diffusion coefficient of $(1.02\pm1.20)\times10^{-9}$ cm^2 s^{-1}. Thus, the mean phycobilisome diffusion coefficient in Δ*rpa*C cells is about twice as high as in the wild-type. However, the very wide range of diffusion coefficients observed in Δ*rpa*C cells makes it uncertain if the difference is significant.

Phycobilisome–reaction centre interactions can be further explored by FRAP in the presence of high osmotic-strength solutions, which stabilise phycobilisome–reaction centre interaction and prevent phycobilisome diffusion [7]. These solutions also inhibit state transitions, so that cells can be locked in either State 1 or State 2 by the appropriate adaptation prior to addition of the buffer [7]. Although the conditions are artificial, the

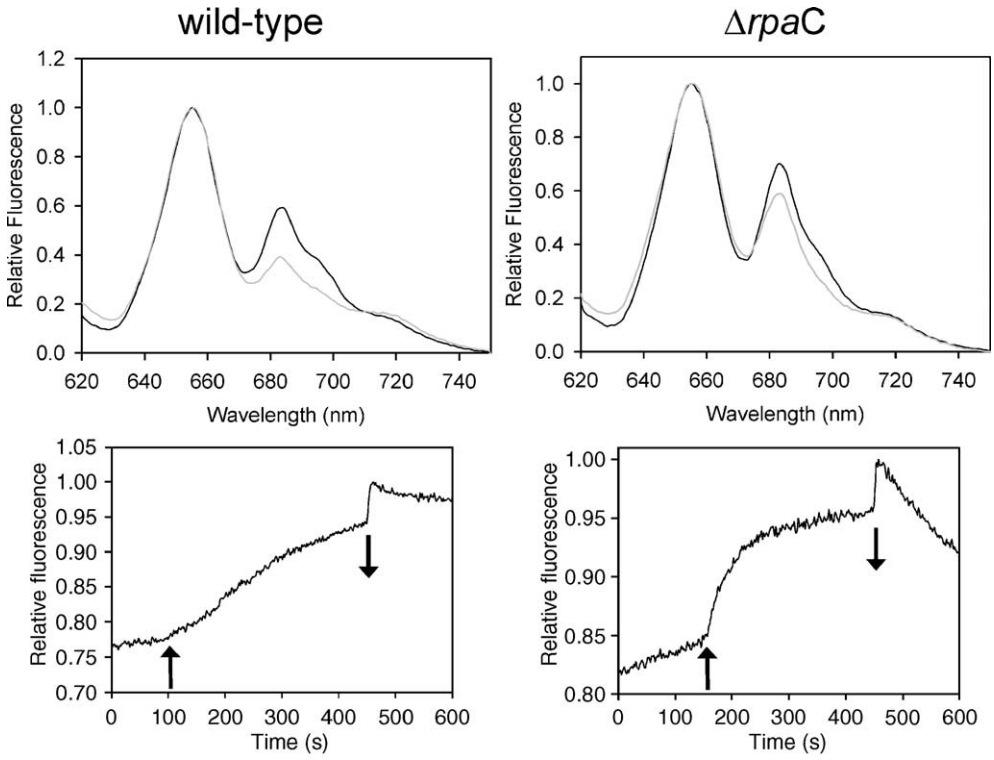

Fig. 3. State transitions in *Synechococcus* 7942 wild-type and Δ*rpa*C. Top: 77K fluorescence emission spectra with excitation at 600 nm (phycocyanin excitation). Spectra are normalised to the phycocyanin emission peak at 654 nm. Black line: cells adapted to State 1. Grey line: cells adapted to State 2. Bottom: fluorescence time-courses at room temperature. Fluorescence was excited with weak, modulated 600 nm light and detected at 680 nm. A red actinic light was added where indicated by the up-arrows and removed where indicated by the down-arrows.

method allows us to perform FRAP measurements on cells specifically adapted to State 1 or to State 2, and thus to compare the interactions of phycobilisomes with Photosystem II and Photosystem I [7]. 77K fluorescence emission spectra (Fig. 4) show that the effect of high osmotic-strength solutions is found in the non-segregated Δ*rpa*C as well as in the wild-type [7], confirming that Δ*rpa*C is capable of state transitions similarly to the wild-type. We carried out FRAP measurements for Δ*rpa*C cells locked in either State 1 or State 2 by exposure to 0.5 M sucrose, a concentration just sufficient to inhibit state transitions [7]. Under these conditions, the mean phycobilisome diffusion coefficient for cells in State 1 was $(4.1\pm0.2)\times10^{-11}$ cm^2 s^{-1}, while for cells in State 2 it was $(3.1\pm0.2)\times10^{-11}$ cm^2 s^{-1}. The corresponding mean diffusion coefficients for wild-type cells under the same conditions are $(6.5\pm0.3)\times10^{-12}$ cm^2 s^{-1} and $(4.7\pm0.3)\times10^{-11}$ cm^2 s^{-1}, respectively [7]. t-tests show that there is no significant difference between wild-type and Δ*rpa*C for cells fixed in State 2 ($P<0.3$), but for cells fixed in State 1 phycobilisomes diffuse on average about 6× faster in Δ*rpa*C, and this difference is significant

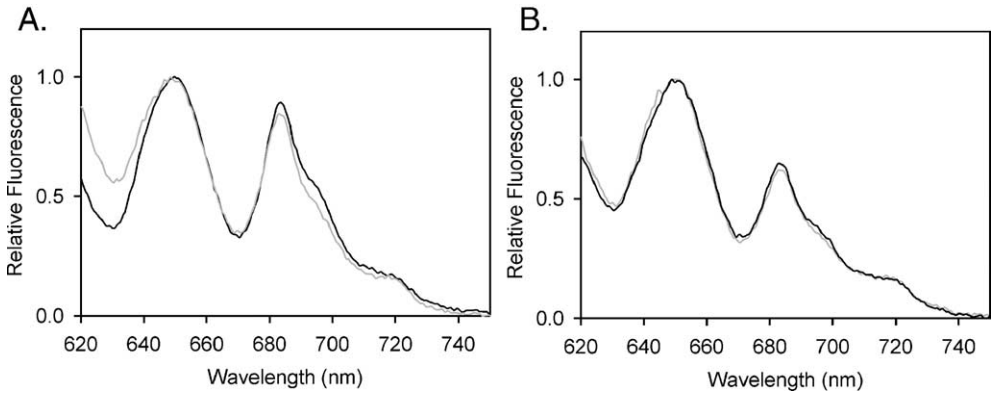

Fig. 4. Fixation of State 1 and State 2 in *Synechococcus* 7942 Δ*rpa*C with 0.5 M sucrose. 77K fluorescence emission spectra with excitation at 600 nm. (A) Cells adapted to State 1 prior to addition of sucrose. (B) Cells adapted to State 2 prior to addition of sucrose. Black lines: cells re-adapted to State 1 conditions after adding sucrose. Grey lines: Cells re-adapted to State 2 conditions after adding sucrose.

($P<0.01$). In State 1, the phycobilisomes interact preferentially with Photosystem II rather than Photosystem I, so this indicates that in Δ*rpa*C the interaction of phycobilisomes with Photosystem II is not so strongly stabilised by 0.5 M sucrose as in the wild-type. Therefore the structural interaction of phycobilisomes with Photosystem II must be perturbed in the non-segregated Δ*rpa*C mutant.

3.7. Excessive rpaC expression is lethal to Synechocystis 6803

Deletion of *rpa*C in *Synechocystis* 6803 leads to specific loss of the phycobilisome component of state transitions [9,11,23]. To further explore the role of *rpa*C in this cyanobacterium, we constructed overexpression mutants (*rpa*C+) in which an additional copy of the *rpa*C gene is inserted into the chromosomal *psb*AII locus, with a downstream spectinomycin resistance marker with the coding sequence in the same orientation. Overexpression mutants were constructed in the wild-type background (*rpa*C+), and in the null mutant in which the native copy of *rpa*C is inactivated (Δ*rpa*C.*rpa*C+). The *psb*AII locus has been previously used for expression of heterologous genes in *Synechocystis* 6803 [24,25]. Expression of this locus is strong and constitutive, but loss of the *psb*AII gene does not appear to affect growth under laboratory conditions, as *Synechocystis* 6803 has a second copy of the gene [24]. Transformants were repeatedly restreaked on spectinomycin-containing plates, and their genotypes were checked with PCR. Primers hybridising within the *psb*AII promoter region, the *rpa*C coding sequence and the spectinomycin resistance cassette were used to confirm the presence of the overexpression construct in the *Synechocystis* 6803 chromosome. Primers hybridising within the *psb*AII promoter and coding regions were used to test for the presence of the wild-type locus. Unexpectedly, we found that the wild-type locus persisted in the transformants (both *rpa*C+ and Δ*rpa*C.*rpa*C+), showing that they could not segregate under a range of illumination conditions in the presence or absence of glucose (not shown). Failure to segregate is not due to loss of the *psb*AII gene, as a *psb*AII null mutant (Δ*psb*AII) segregated easily (not shown). Therefore, the failure to segregate shows that *rpa*C expression levels that would be obtained in a fully segregated *rpa*C+ or Δ*rpa*C.*rpa*C+ mutant must be lethal.

3.8. Overexpression of rpaC perturbs phycobilisome–Photosystem II energy transfer in Synechocystis 6803

The partially-segregated *Synechocystis* *rpa*C+ and Δ*rpa*C.*rpa*C+ mutants showed a number of striking phenotypic characteristics. These effects were not seen in Δ*psb*AII, which contains the antibiotic resistance cassette, but not the *rpa*C gene, inserted into the *psb*AII locus. Therefore, the phenotypic effects must result from overexpression of *rpa*C. Table 2 compares growth rates for Δ*rpa*C.*rpa*C+ with those for Δ*psb*AII and Δ*rpa*C as controls. Growth of Δ*rpa*C.*rpa*C+ was slower than that of the other strains at all intensities of white light (Table 2). However, Δ*rpa*C.*rpa*C+ was not disadvantaged compared to the other strains under weak blue illumination, which is not absorbed by the phycobilisomes (Table 2). This suggests that the reduced growth rate is due to a defect in phycobilisome light-harvesting. 77K fluorescence emission spectra with chlorophyll excitation show greatly increased PS II emission relative to PS I, as compared to Δ*psb*AII as a control. This is particularly the case when cells are grown in low light (Fig. 5). Spectra for wild-type are similar to Δ*psb*AII, and Δ*psb*AII shows no other obvious phenotypic differences from the wild-type (not shown). Δ*rpa*C.*rpa*C+ shows much lower chlorophyll and PS I per cell (Table 1), indicating that PS I is down-regulated. PS I biosynthesis is under redox control, which acts to correct imbalances in PS II and PS I excitation [26]. Thus, the down-regulation of PS I may be a response to defects in PS II light-harvesting. 77K fluorescence emission spectra with phycobilisome excitation (Fig. 6) show elevated fluorescence from allophycocyanin in the phycobilisome core at 665 nm, suggesting a perturbation in energy transfer, either within the phycobi-

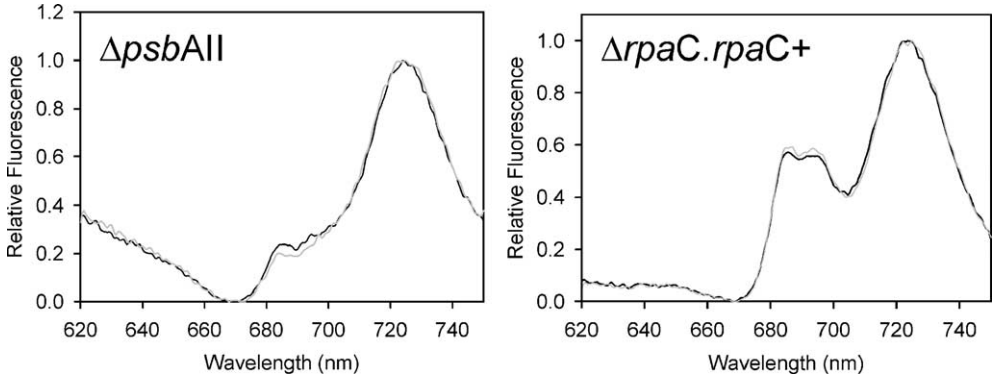

Fig. 5. 77K fluorescence emission spectra for cells of *Synechocystis* 6803 Δ*psb*AII and Δ*rpa*C.*rpa*C+ grown under low light, with excitation at 435 nm (chlorophyll *a* excitation). Black lines: cells adapted to State 1 conditions before freezing. Grey lines: cells adapted to State 2 conditions before freezing. Spectra normalised to the Photosystem I emission at 725 nm.

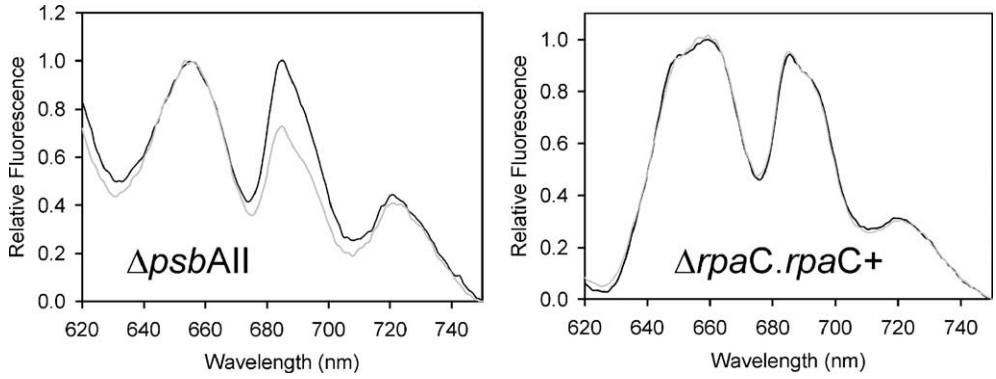

Fig. 6. 77K fluorescence emission spectra for cells of *Synechocystis* 6803 Δ*psb*AII and Δ*rpa*C.*rpa*C+ grown under low light, with excitation at 600 nm (phycocyanin excitation). Black lines: cells adapted to State 1 conditions before freezing. Grey lines: cells adapted to State 2 conditions before freezing. Spectra normalised to phycocyanin emission at 654 nm.

lisome core or from phycobilisomes to reaction centres. The same effect was seen when *rpa*C was overexpressed in the wild-type background (*rpa*C+) (not shown). Δ*rpa*C cells are incapable of state transitions [9]. We found that overexpression of *rpa*C in this background (Δ*rpa*C.*rpa*C+) C+) did not restore the ability to perform state transitions, as judged from 77K fluorescence spectra (Fig. 6) and room temperature fluorescence timecourses (not shown).

4. Discussion

4.1. RpaC is not a state transition signal transducer

A *Synechocystis* 6803 *rpa*C null mutant is incapable of performing state transitions [9]. This appears to be a very specific phenotype, as it is not accompanied by any other obvious defects in photosynthetic light-harvesting or electron transport. As judged from 77K fluorescence emission spectra, *Synechocystis* 6803 Δ*rpa*C is permanently in State 1, the state in which phycobilisomes preferentially interact with PS II [9]. These results suggested that *rpa*C may be a novel signal transduction component required for state transitions [9]. The subsequent publication of several more cyanobacterial genome sequences revealed that *rpa*C is a highly conserved gene in cyanobacteria [11]. However, no orthologs have been detected in green plants, consistent with a specific role in controlling the interaction of phycobilisomes with reaction centres [11]. In this study we have tested the idea that the *rpa*C gene product may be a state transition signal transducer, first by deleting the ortholog in a second cyanobacterium, *Synechococcus* 7942, and then by overexpressing *rpa*C in *Synechocystis* 6803. In both cases, the results were unexpected.

Synechocystis 6803 Δ*rpa*C does not perform state transitions but is disadvantaged compared to the wild-type only under very weak illumination [9,11]. This shows that state transitions are not essential for cyanobacteria, although they confer a slight advantage under certain growth conditions. This also appears to be the case in green plants [27]. We identified a *Synechococcus* 7942 gene strongly homologous to *Synechocystis* 6803 *rpa*C. If *rpa*C were a state transition signal transducer, we would expect that the *Synechococcus* 7942 *rpa*C mutant would only be disadvantaged under weak illumination [9,11]. However, we found that *Synechococcus* 7942 Δ*rpa*C was unable to segregate under any of the conditions tested, showing that complete loss of the gene is always lethal in this cyanobacterium. This suggests that, despite the phenotype observed in *Synechocystis* 6803 Δ*rpa*C, *rpa*C does not have a specific role in state transitions. This is confirmed by the phenotype of a *Synechocystis* 6803 mutant in which *rpa*C is overexpressed. Overexpression of *rpa*C in the Δ*rpa*C background does not restore the ability to perform state transitions. The overexpressor is unable to segregate completely, indicating that *Synechocystis* 6803 can only tolerate a certain level of *rpa*C expression. The overexpressor also shows perturbed light-harvesting and an increased ratio of PS II/PS I. None of these results is consistent with a simple, specific role for RpaC in mediating the signal transduction pathway of state transitions. It remains very possible that state transitions generally cannot occur in the absence of RpaC. The *Synechococcus* 7942 Δ*rpa*C mutant is capable of state transitions but is non-segregated and retains significant levels of *rpa*C expression. Therefore, we cannot be sure if state transitions also depend on *rpa*C in this cyanobacterium. However, our results indicate a more general role for RpaC in mediating phycobilisome–reaction centre interaction.

4.2. RpaC may be involved in controlling the stability of phycobilisome–Photosystem II interaction

The phenotypes of the fully-segregated *Synechocystis* 6803 Δ*rpa*C mutant [9] and the non-segregated *Synechococcus* 7942 Δ*rpa*C mutant are superficially rather different. *Synechocystis* 6803 Δ*rpa*C appears to be permanently in State 1, suggesting that the interaction between phycobilisomes and PS II is stabilised [9]. By contrast, *Synechococcus* 7942 Δ*rpa*C shows weaker phycobilisome–PS II

interaction, as judged from fluorescence spectra and FRAP measurements. However, what both mutants have in common is a phycobilisome–PS II interaction that is perturbed in some way, and this is also seen in *Synechocystis* 6803 *rpa*C+. All these results suggest that the precise level of *rpa*C expression is important for appropriate interaction of phycobilisomes with PS II.

4.3. Working hypothesis for the role of RpaC

The structural basis of the interaction between phycobilisomes and reaction centres is not clear. A large linker polypeptide in the phycobilisome core, ApcE (sometimes known as the "anchor polypeptide") appears to play a critical role [28]. High-resolution structural information is now available for cyanobacterial Photosystem II [29] and Photosystem I [30] but the structure of ApcE is not known, so only crude modelling of phycobilisome–reaction centre interaction is possible [31]. FRAP measurements show that the interaction between phycobilisomes and reaction centres in vivo must be rather weak and unstable [5,6]. Energy transfer and mutagenesis studies strongly suggest that the phycobilisome cores can interact directly with Photosystem I as well as Photosystem II [2,22]. This is remarkable because the cytoplasmic surfaces of Photosystem II and Photosystem I have very different topologies [29,30]. Reconstitution studies have shown the ability of phycobilisomes to bind to lipid vesicles and heterologous reaction centres [32]. These findings suggest that the interaction of phycobilisomes with membrane complexes is rather non-specific.

As a working hypothesis, we propose that RpaC is a structural component of the phycobilisome–Photosystem II complex (Fig. 7). RpaC acts to ensure that the binding of phycobilisomes to Photosystem II is neither too stable nor too unstable. Excessive stability of the phycobilisome–Photosystem II complex will lead to inability to regulate light-harvesting [7,8]. Excessive instability of the complex will lead to inefficient light-harvesting, which will be deleterious at low light intensities and may be dangerous at high light intensities. We suggest that RpaC plays the same functional role in all cyanobacteria, consistent with its highly-conserved sequence [11]. The phenotypic differences between the *Synechocystis* 6803 and *Synechococcus* 7942 null mutants may be due to different modes of phycobilisome–Photosystem II interaction in the absence of RpaC. In *Synechocystis* 6803, deletion of *rpa*C appears to result in stabilisation of phycobilisome–Photosystem II interaction, leading to loss of state transitions [9]. In *Synechococcus* 7942, reduction in *rpa*C gene copy number, with concomitant lower *rpa*C transcript levels, leads to weaker phycobilisome–Photosystem II interaction. The different effect in *Synechococcus* 7942 may explain why *Synechococcus* 7942 Δ*rpa*C is unable to segregate. The structural basis of the different responses in *Synechocystis* 6803 and *Synechococcus* 7942 may lie in their somewhat different phycobilisome core structures: *Synechocystis* 6803 has three core substructures whereas *Synechococcus* 7942 has two [33]. Overexpression of *rpa*C may lead to accumulation of RpaC in the membrane that is not complexed to Photosystem II. We suggest that the perturbation of light-harvesting in *Synechocystis* 6803 *rpa*C+ and Δ*rpa*C.*rpa*C+ may be a consequence of interaction of phycobilisomes with free RpaC subunits (Fig. 7). This effect may explain why excessive expression of *rpa*C is lethal.

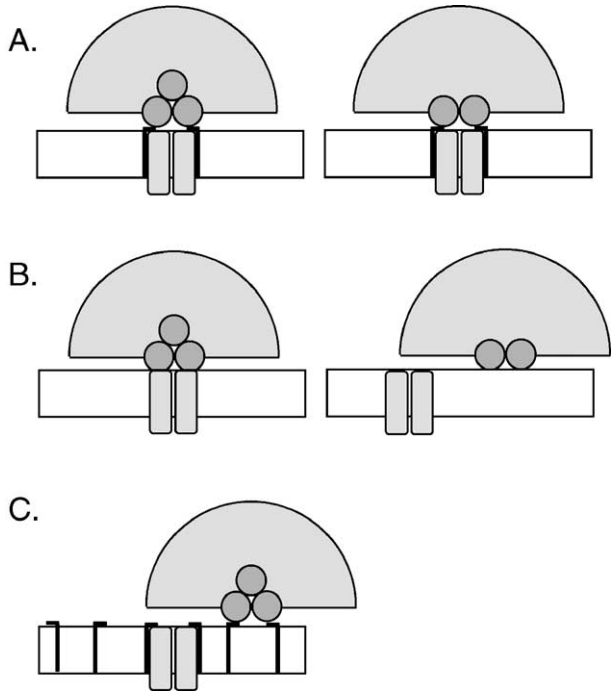

Fig. 7. Working hypothesis for the function of RpaC. RpaC subunits shown in black, Photosystem II complexes shown as dimers in the membrane, phycobilisomes shown as fan-shaped complexes on the membrane surface with either three core substructures (*Synechocystis* 6803) or two (*Synechococcus* 7942). (A) RpaC maintains correct interaction between phycobilisomes (shown as fan shaped-complexes on the thylakoid membrane surface) and Photosystem II (dimers in the membrane). (B) In the absence of RpaC, phycobilisome–Photosystem II complexes are stabilised in *Synechocystis* 6803 but destabilised in *Synechococcus* 7942. (C) Overexpression of RpaC leads to free subunits in the membrane and light-harvesting is perturbed due to interaction of phycobilisomes with the free subunits.

Further studies will be needed to test the model illustrated in Fig. 7. In particular, it will be important to use important to use epitope-tagging to test the idea that RpaC is a structural component of the phycobilisome–Photosystem II complex.

Acknowledgements

SJ is supported by a BBSRC research studentship. Funded by BBSRC and Wellcome Trust grants to CWM. We thank Peter Rich (University College London) for the use of his flash photometer, Peter Nixon (Imperial College London) for the gift of the construct used to make the

Synechocystis 6803 Δ*psb*AII mutant and Susan Golden (Texas A and M University) and US Department of Energy Joint Genome Institute for the use of *Synechococcus* 7942 sequence data prior to publication.

References

[1] A.R. Grossman, M.R. Schaefer, G.G. Chiang, J.L. Collier, The phycobilisome, a light-harvesting complex responsive to environmental conditions, Microbiol. Rev. 57 (1993) 725–749.
[2] C.W. Mullineaux, Excitation energy transfer from phycobilisomes to photosystem I in a cyanobacterial mutant lacking photosystem II, Biochim. Biophys. Acta 1184 (1994) 71–77.
[3] M.K. Ashby, C.W. Mullineaux, The role of ApcD and ApcF in energy transfer from phycobilisomes to PSI and PSII in a cyanobacterium, Photosynth. Res. 61 (1999) 169–179.
[4] M.G. Rakhimberdieva, V.A. Boichenko, N. Karapetyan, I.N. Stadnichuk, Interaction of phycobilisomes with photosystem II dimers and photosystem I monomers and trimers in the cyanobacterium *Spirulina platensis*, Biochemistry 40 (2001) 15780–15788.
[5] C.W. Mullineaux, M.J. Tobin, M.R. Jones, Mobility of photosynthetic complexes in thylakoid membranes, Nature 390 (1997) 421–424.
[6] M. Sarcina, M.J. Tobin, C.W. Mullineaux, Diffusion of phycobilisomes on the thylakoid membranes of the cyanobacterium *Synechcoccus* 7942. Effects of phycobilisome size, temperature and membrane lipid composition, J. Biol. Chem. 276 (2001) 46830–46834.
[7] S. Joshua, C.W. Mullineaux, Phycobilisome diffusion is required for light-state transitions in cyanobacteria, Plant Physiol. 135 (2004) 2112–2119.
[8] S. Joshua, S. Bailey, N.H. Mann, C.W. Mullineaux, Involvement of phycobilisome diffusion in energy quenching in cyanobacteria. Plant Physiol. 138 (3) (2005).
[9] D. Emlyn-Jones, M.K. Ashby, C.W. Mullineaux, A gene required for the regulation of photosynthetic light-harvesting in the cyanobacterium *Synechocystis* 6803, Mol. Microbiol. 33 (1999) 1050–1058.
[10] Y. Nakamura, T. Kaneko, S. Tabata, CyanoBase, the genome database for *Synechocystis* sp. strain PCC6803: status for the year 2000, Nucleic Acids Res. 28 (2000) 72.
[11] C.W. Mullineaux, D. Emlyn-Jones, State transitions: an example of acclimation to low-light stress, J. Exp. Bot. 56 (2005) 389–393.
[12] C.W. Mullineaux, M. Sarcina, Probing the dynamics of photosynthetic membranes with fluorescence recovery after photobleaching, Trends Plant Sci. 7 (2002) 237–240.
[13] R.W. Castenholz, Culturing methods for cyanobacteria, in: L. Packer, A.N. Glazer (Eds.), Methods in Enzymology, vol. 167, Academic Press, San Diego, 1988, pp. 68–93.
[14] J. Sambrook, E.F. Fritsch, T. Maniatis, Molecular Cloning: a Laboratory Manual, 2nd ed., Cold Spring Harbor Laboratory Press, Cold Spring Harbor, NY, 1989.
[15] R.D. Porter, DNA transformation, in: L. Packer, A.N. Glazer (Eds.), Methods in Enzymology, vol. 167, Academic Press, San Diego, 1988, pp. 68–93.
[16] P. Prentki, H.M. Krisch, In vitro insertional mutagenesis with a selectable DNA fragment, Gene 29 (1984) 303–313.
[17] R.J. Porra, W.A. Thompson, P.E. Kriedemann, Determination of accurate extinction coefficients and simultaneous equations for assaying chlorophylls *a* and *b* extracted with four different solvents: verification of the concentration of chlorophyll standards by atomic absorption spectroscopy, Biochim. Biophys. Acta 975 (1989) 384–394.
[18] J. Myers, J.-R. Graham, R.T. Wang, Light-harvesting in *Anacystis nidulans* studied in pigment mutants, Plant Physiol. 66 (1980) 1144–1149.
[19] W.S. Chow, A.B. Hope, J.M. Anderson, A reassessment of the use of herbicide binding to measure photosystem-II reaction centers in plant thylakoids, Photosynth. Res. 24 (1990) 109–113.
[20] T. Hiyama, B. Ke, Difference spectra and extinction coefficients of P700, Biochim. Biophys. Acta 267 (1972) 160–171.
[21] M. Sarcina, C.W. Mullineaux, Mobility of the IsiA chlorophyll-binding protein in cyanobacterial thylakoid membranes, J. Biol. Chem. 279 (2004) 36514–36518.
[22] M.K. Ashby, C.W. Mullineaux, The role of ApcD and ApcF in energy transfer from phycobilisomes to PS I and PS II in a cyanobacterium, Photosynth. Res. 61 (1999) 169–179.
[23] M.D. McConnell, R. Koop, S. Vasil'ev, D. Bruce, Regulation of the distribution of chlorophyll and phycobilin-absorbed excitation energy in cyanobacteria. A structure-based model for the light state transition, Plant Physiol. 130 (2002) 1201–1212.
[24] D. Lagarde, L. Beuf, W. Vermaas, Increased production of zeaxanthin and other pigments by application of genetic engineering techniques to *Synechocystis* sp. strain PCC 6803, Appl. Environ. Microbiol. 66 (2000) 64–72.
[25] E. Spence, M. Sarcina, N. Ray, S.G. Møller, C.W. Mullineaux, C. Robinson, Membrane-specific targeting of green fluorescent protein by the Tat pathway in the cyanobacterium *Synechocystis* PCC6803. Mol. Microbiol. 48, 1481–1489.
[26] H. Li, L.A. Sherman, A redox-responsive regulator of photosynthesis gene expression in the cyanobacterium *Synechocystis* sp strain PCC 6803, J. Bacteriol. 182 (2000) 4268–4277.
[27] S. Bellafiore, F. Barneche, G. Peltier, J.-D. Rochaix, State transitions and light adaptation require chloroplast thylakoid protein kinase STN7, Nature 433 (2005) 892–895.
[28] J. Houmard, V. Capuano, M.V. Colombano, T. Coursin, N. Tandeau de Marsac, Molecular characterisation of the terminal energy acceptor of cyanobacterial phycobilisomes, Proc. Natl. Acad. Sci. U. S. A. 87 (1990) 2152–2156.
[29] A. Zouni, H.-T. Witt, J. Kern, P. Fromme, N. Krauß, W. Saenger, P. Orth, Crystal structure of photosystem II from *Synechococcus elongatus* 3.8 Å resolution, Nature 409 (2001) 739–743.
[30] P. Jordan, P. Fromme, H.T. Witt, O. Klukas, W. Saenger, N. Krauß, Three-dimensional structure of cyanobacterial photosystem I at 2.5 angstrom resolution, Nature 411 (2001) 909–917.
[31] J. Barber, E.P. Morris, P.C.A. da Fonseca, Interaction of the allophycocyanin core complex with photosystem II, Photochem. Photobiol. Sci. 2 (2003) 536–541.
[32] D. Kirilovsky, I. Ohad, Functional assembly in vitro of phycobilisomes with isolated Photosystem-II particles of eukaryotic chloroplasts, J. Biol. Chem. 261 (1986) 2317–2323.
[33] A.N. Glazer, Phycobilisome—A macromolecular complex optimized for light-energy transfer, Biochim. Biophys. Acta 768 (1984) 29–51.